

Growth of $\text{In}_{0.25}\text{Ga}_{0.75}\text{As}$ quantum dots on GaP utilizing a GaAs interlayer

Cite as: Appl. Phys. Lett. **101**, 223110 (2012); <https://doi.org/10.1063/1.4768294>

Submitted: 09 July 2012 • Accepted: 06 November 2012 • Published Online: 27 November 2012

G. Stracke, A. Glacki, T. Nowozin, et al.



View Online



Export Citation

ARTICLES YOU MAY BE INTERESTED IN

[Indirect and direct optical transitions in \$\text{In}_{0.5}\text{Ga}_{0.5}\text{As}/\text{GaP}\$ quantum dots](#)

Applied Physics Letters **104**, 123107 (2014); <https://doi.org/10.1063/1.4870087>

[Spatial structure of \$\text{In}_{0.25}\text{Ga}_{0.75}\text{As}/\text{GaAs}/\text{GaP}\$ quantum dots on the atomic scale](#)

Applied Physics Letters **102**, 123102 (2013); <https://doi.org/10.1063/1.4798520>

[Atomic structure and optical properties of InAs submonolayer depositions in GaAs](#)

Journal of Vacuum Science & Technology B **29**, 04D104 (2011); <https://doi.org/10.1116/1.3602470>

 QBLOX



1 qubit

Shorten Setup Time

Auto-Calibration

More Qubits

Fully-integrated

Quantum Control Stacks

Ultrastable DC to 18.5 GHz

Synchronized <<1 ns

Ultralow noise



100s qubits

[visit our website >](#)

Growth of $\text{In}_{0.25}\text{Ga}_{0.75}\text{As}$ quantum dots on GaP utilizing a GaAs interlayer

G. Stracke,^{a)} A. Glacki, T. Nowozin, L. Bonato, S. Rodt, C. Prohl, A. Lenz, H. Eisele, A. Schliwa, A. Strittmatter, U. W. Pohl, and D. Bimberg^{b)}

Institut für Festkörperphysik, Technische Universität Berlin, Hardenbergstrasse 36, 10623 Berlin, Germany

(Received 9 July 2012; accepted 6 November 2012; published online 27 November 2012)

Coherent $\text{In}_{0.25}\text{Ga}_{0.75}\text{As}$ quantum dots (QDs) are realized on GaP(001) substrates by metalorganic vapor phase epitaxy in the Stranski-Krastanow mode utilizing a thin GaAs interlayer prior to $\text{In}_{0.25}\text{Ga}_{0.75}\text{As}$ deposition. Luminescence is observed between 2.0 eV and 1.83 eV, depending on the thickness of the $\text{In}_{0.25}\text{Ga}_{0.75}\text{As}$ layer. The critical thickness for the two-dimensional to three-dimensional transition of the layer is determined to 0.75 to 1.0 monolayers. A mean activation energy of 489 meV for holes captured by $\text{In}_{0.25}\text{Ga}_{0.75}\text{As}$ quantum dots is measured by deep-level transient spectroscopy, yielding a hole storage time of 3 μs at room temperature. © 2012 American Institute of Physics. [<http://dx.doi.org/10.1063/1.4768294>]

The growth of self-assembled quantum dots (QDs) has been studied extensively in material systems such as In(Ga)As on GaAs.¹ Comparatively, little work has been presented hitherto on In(Ga)As QDs embedded in a GaP matrix.^{2,3} Recently, InGaAs QDs on GaP have been studied with respect to their suitability as active medium for opto-electronic devices.^{4,5} A completely different prospective application of such QDs is the fabrication of nanomemory cells as predicted by Marent *et al.*⁶ Such QD memory cells promise to combine the fast write and erase times of a DRAM with the non-volatility of a Flash memory. InAs QDs embedded in a GaAs matrix yield a hole storage time of 0.5 ns at room temperature (Ref. 7). In order to achieve longer storage times, higher localization energies of the charge carriers inside the QDs are needed. Pedesseau *et al.*⁸ calculated the valence band discontinuity of strained InAs in GaP to 0.93 eV. Compared to InAs QDs in GaAs, which have a valence band discontinuity of only 0.25 eV,⁹ considerably longer hole storage times are expected for InAs QDs in GaP. Such structures additionally offer the potential for integration with Si, since GaP and Si have almost the same lattice constant. Self-organized QDs can be formed via the Stranski-Krastanow (SK) growth mode¹⁰ if the release of elastic energy upon forming three-dimensional islands surpasses the energy required to create new surfaces and edges.¹¹ The formation energies of relevant surface reconstructions of GaP(001) surfaces are significantly higher than those of GaAs(001) surfaces,^{12,13} potentially inhibiting the QD formation. In this study, different growth modes of $\text{In}_x\text{Ga}_{1-x}\text{As}$ layers are realized by growing on P-terminated surfaces and on As-terminated surfaces. We analyze the hole localization within the QD layer by deep-level transient spectroscopy (DLTS) measurements and estimate the storage time for holes in such QDs.

The samples are grown in a horizontal Aixtron 200 MOVPE reactor using GaP(001) substrates and H_2 as carrier gas. First, 500 nm thick undoped GaP buffer layers are grown at a substrate temperature of 750 °C. The temperature is then lowered to 500 °C for the growth of GaAs and $\text{In}_{0.25}\text{Ga}_{0.75}\text{As}$

layers. After deposition of the $\text{In}_{0.25}\text{Ga}_{0.75}\text{As}$ layer, a growth interruption (GRI) ranging from 1 s to 100 s without any precursor supply is applied, followed by the deposition of a 6 nm thick GaP cap layer. Additional GaP layers above the QDs are grown at 600 °C.

Atomic force micrographs (AFMs) given in Figures 1(a)–1(f) demonstrate that the surface termination is decisive for the formation of InGaAs QDs on GaP(001) substrates. For comparison with In(Ga)As/GaAs QDs, Figure 1(a) shows the typical morphology of a 2.4 monolayer (ML) thick $\text{In}_{0.83}\text{Ga}_{0.17}\text{As}$ layer capped by 6 nm GaAs. The sample was grown at 490 °C on a GaAs(001) substrate. For a GRI time of 180 s, islands with a density of $1.4 \times 10^{10} \text{ cm}^{-2}$ and 8 nm to 10 nm height are observed. In contrast, on GaP(001) substrates, a flat surface without any noticeable QD morphology is found for the same growth conditions of $\text{In}_{0.83}\text{Ga}_{0.17}\text{As}$ capped with 6 nm GaP (see Figure 1(b)). The flat islands visible on the surface are only 1 ML high and result from a change of the GaP growth mode at low temperatures as verified in Figures 1(e) and 1(f). In Figure 1(e), the surface of a 500 nm thick GaP buffer layer grown at 750 °C shows perfectly smooth terraces proving a step-flow growth. A 6 nm thick GaP layer grown at 500 °C directly on the GaP buffer layer leads to small 1 ML high islands on the terraces (Figure 1(f)). Obviously, at low growth temperatures of about 500 °C, the step-flow mode of the GaP growth is no longer preserved. It is noted that the lattice mismatch of $\text{In}_{0.83}\text{Ga}_{0.17}\text{As}$ layers on GaP of 9.9% significantly exceeds that of $\text{In}_{0.83}\text{Ga}_{0.17}\text{As}$ layers on GaAs, being about 5.9%. Still, the SK growth mode of InGaAs QDs on GaP(001) substrates is not initiated. Hence, a reduction of the surface energy is necessary in order to enable QD formation via the SK growth mode. For that purpose, 3 ML of GaAs are deposited on the GaP buffer layer prior to the growth of the InGaAs layer. In order to match the lattice mismatch of the InGaAs layer on GaP(001) with respect to that of the $\text{In}_{0.83}\text{Ga}_{0.17}\text{As}$ layer on GaAs(001) shown in Figure 1(a), the indium content is reduced to $x_{\text{In}} = 25\%$ corresponding to a lattice mismatch of 5.6%. Figures 1(c) and 1(d) show AFM images of 2.3 ML $\text{In}_{0.25}\text{Ga}_{0.75}\text{As}$ grown on top of 3 ML GaAs on a GaP(001) substrate. GRIs of 10 s and 100 s were, respectively, applied,

^{a)}gernot.stracke@tu-berlin.de.

^{b)}Also at King Abdulaziz University, Saudi Arabia.

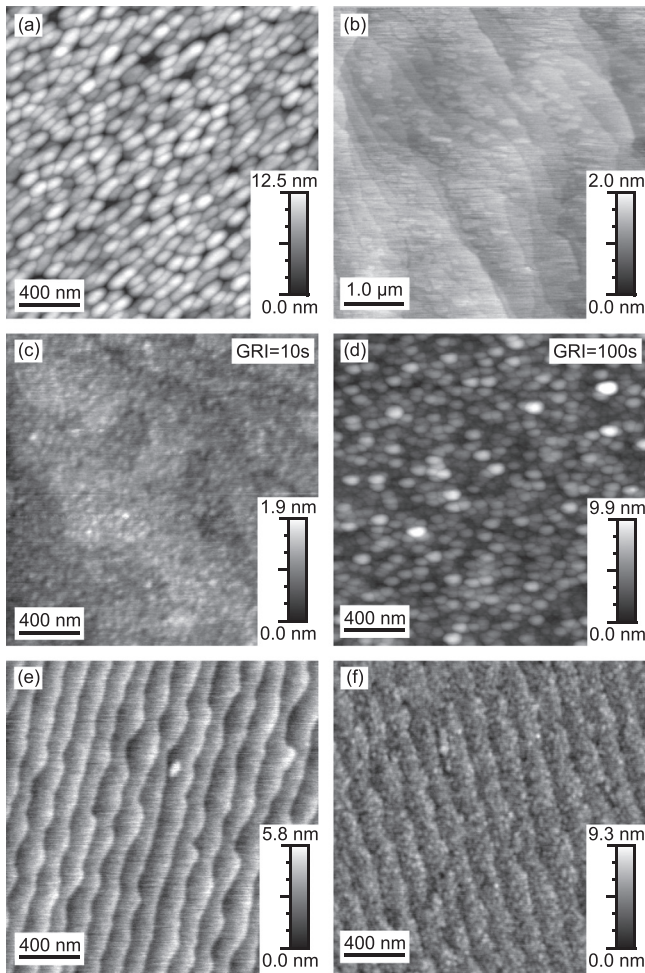


FIG. 1. (a) and (b) AFM images of 2.4 ML $\text{In}_{0.83}\text{Ga}_{0.17}\text{As}$ deposited on GaAs (a) and on GaP (b) with GRI = 180 s for both samples, and (c) and (d) 2.3 ML $\text{In}_{0.25}\text{Ga}_{0.75}\text{As}$ deposited on a 3 ML GaAs interlayer on GaP, GRI = 10 s (c) and 100 s (d). The samples are capped with 6 nm GaAs (a) or GaP (b)–(d). (e) and (f) Reference samples of 500 nm GaP grown at 750 °C (e), and an additional 6 nm GaP layer grown on top at 500 °C (f).

followed by 6 nm GaP cap layers. Now, the surface shows a QD-like morphology already after a GRI of 10 s. Small islands with a height of 0.5 nm to 1 nm (2–4 ML) and a density of $1.5 \times 10^{10} \text{ cm}^{-2}$ are visible. For an extended GRI of 100 s, the islands increase in size to a height of 4 nm to 8 nm and a lateral extension of 70 nm to 100 nm with a density of $1.2 \times 10^{10} \text{ cm}^{-2}$. It must be noted that the total elastic energy of 3 ML GaAs + 2.3 ML $\text{In}_{0.25}\text{Ga}_{0.75}\text{As}$ on GaP, for which QD formation is observed, is smaller than that of 2.4 ML $\text{In}_{0.83}\text{Ga}_{0.17}\text{As}$ on GaP, which grows two-dimensionally. From these results, QD formation due to a reduction of the surface energy of GaP(001) substrates by insertion of a few ML GaAs is concluded. It is noted that a nominal deposition thickness of below 3 ML GaAs does not enable the SK growth mode. This can be due to phosphorus to arsenic exchange processes at the growth interface, which result in a reduced amount of As at the interface to the $\text{In}_x\text{Ga}_{1-x}\text{As}$ layer.

Figure 2 shows a cross-sectional scanning tunneling micrograph (XSTM) of a buried $\text{In}_{0.25}\text{Ga}_{0.75}\text{As}/\text{GaAs}/\text{GaP}$ QD. The nominal $\text{In}_{0.25}\text{Ga}_{0.75}\text{As}$ coverage for this sample is 2.0 ML, and the GRI is set to 10 s. The QD has the shape of a truncated pyramid with a base length of 12 nm and a height

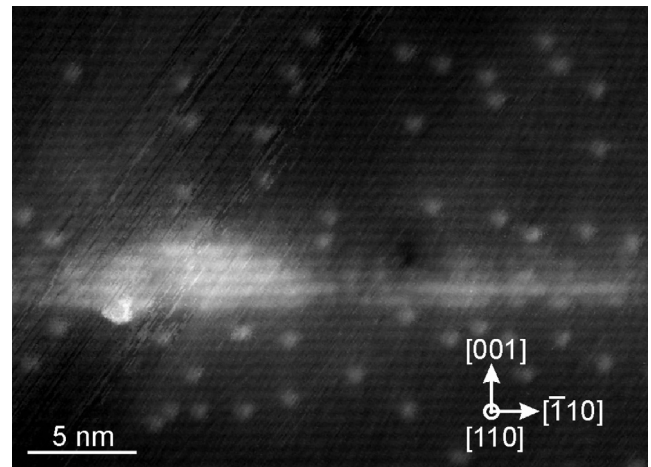


FIG. 2. XSTM image of a buried truncated pyramid shaped QD, formed from 2 ML $\text{In}_{0.25}\text{Ga}_{0.75}\text{As}/3 \text{ ML GaAs}/\text{GaP}(001)$. The image was taken at a sample bias of $V_t = -3.0 \text{ V}$ and a tunneling current of $I_t = 30 \text{ pA}$. The QD has a base length of 12 nm and a height of 10 ML (2.7 nm). A wetting layer is clearly visible. The bright spots are due to adsorbed ad-atoms at the cleavage surface.

of 10 ML (2.7 nm). A wetting layer is clearly visible, proving the SK growth mode. A truncated reversed-cone stoichiometric profile¹⁴ is observed for the QD, where the deposited 3 ML GaAs, and $\text{In}_{0.25}\text{Ga}_{0.75}\text{As}$ cannot be distinguished as two distinct layers. The QD density is found to be in the range of $1.0 \times 10^{11} \text{ cm}^{-2}$ to $2.9 \times 10^{11} \text{ cm}^{-2}$, in agreement with the value determined from the AFM image Figure 3(d).

For determining the critical $\text{In}_{0.25}\text{Ga}_{0.75}\text{As}$ coverage for the 2D–3D transition, a series of samples with varying $\text{In}_{0.25}\text{Ga}_{0.75}\text{As}$ layer thickness is grown without the GaP cap layer, which might conceal small QDs or QD precursors. Figure 3(a) shows an AFM image of the surface of a 3 ML thick GaAs layer on GaP. Similar to the low-temperature GaP layer (Figure 1(f)), terraces with 1 ML-high islands are

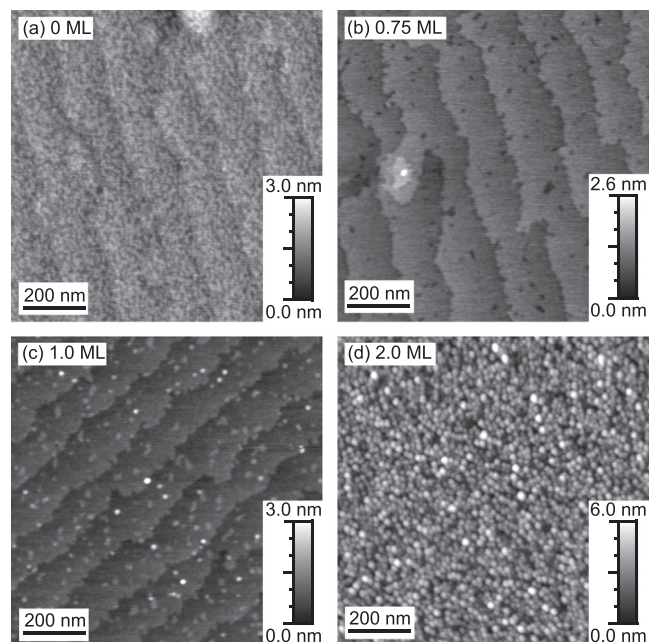


FIG. 3. AFM images of uncapped samples with various layer thickness. (a) Only the 3 ML GaAs interlayer, (b) 0.75 ML, (c) 1.0 ML, and (d) 2.0 ML $\text{In}_{0.25}\text{Ga}_{0.75}\text{As}$ on top of the GaAs interlayer.

observed indicating a 2D-nucleation growth mode. Depositing 0.75 ML of $\text{In}_{0.25}\text{Ga}_{0.75}\text{As}$ on top of the 3 ML GaAs yields a smooth two-dimensional surface with few 1 ML deep pits as shown in Figure 3(b). At an $\text{In}_{0.25}\text{Ga}_{0.75}\text{As}$ thickness of 1 ML, the 2D-3D transition is exceeded (Figure 3(c)). Besides 1 ML high islands, QDs 1.0 nm to 1.8 nm high and 23 nm to 28 nm in diameter are formed with a density of $1 \times 10^9 \text{ cm}^{-2}$. Figure 3(d) shows fully developed, 1.5 nm to 4.0 nm high QDs with 22 nm to 39 nm diameter, and a density of $1.3 \times 10^{11} \text{ cm}^{-2}$. These QDs form after deposition of 2 ML $\text{In}_{0.25}\text{Ga}_{0.75}\text{As}$. It should be noted that AFM typically overestimates the lateral QD size due to the convolution of the sample surface with the AFM tip. Nevertheless, according to this result, the 2D-3D transition occurs between a nominal $\text{In}_{0.25}\text{Ga}_{0.75}\text{As}$ coverage of 0.75 ML and 1.0 ML. From theoretical calculations of the strain energy in the wetting layer,¹⁵ a critical layer thickness between 0.72 ML and 1.04 ML is expected, if similar surface energies for the InAs/GaAs and the InGaAs/GaAs/GaP systems are assumed. This is in excellent agreement with the critical thickness observed here.

In order to evaluate optical properties of the QDs, cathodoluminescence (CL) spectra are taken at a temperature of 5 K for a set of samples with $\text{In}_{0.25}\text{Ga}_{0.75}\text{As}$ thicknesses ranging from 0.0 ML to 2.0 ML on 3 ML GaAs (Figure 4). After GaAs and $\text{In}_{0.25}\text{Ga}_{0.75}\text{As}$ deposition, a GRI of 10 s is applied. The QDs are then capped with 6 nm GaP at 500 °C and 150 nm GaP at 600 °C. The sample containing only 3 ML GaAs solely shows a double luminescence peak at 2.03 eV and 2.0 eV. Upon deposition of ≤ 0.7 ML $\text{In}_{0.25}\text{Ga}_{0.75}\text{As}$ (below critical layer thickness), two luminescence peaks at 2.0 eV and 1.97 eV are observed. At 1 ML $\text{In}_{0.25}\text{Ga}_{0.75}\text{As}$ thickness, a long-wavelength shift to 1.93 eV and 1.90 eV, respectively, occurs. The shift coincides with the QD formation seen in AFM (Figure 3). Increasing the $\text{In}_{0.25}\text{Ga}_{0.75}\text{As}$ thickness further to 1.5 ML shifts the luminescence to 1.83 eV, indicating the formation of larger QDs. At an $\text{In}_{0.25}\text{Ga}_{0.75}\text{As}$ thickness of 2.0 ML, the luminescence intensity degrades strongly. This is a clear indication for the formation of defects and relaxed clusters. The origin of the double

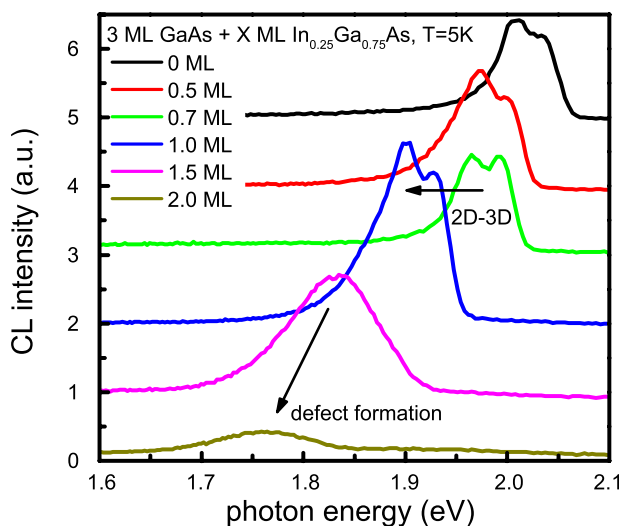


FIG. 4. CL spectra taken at 5 K from samples with various $\text{In}_{0.25}\text{Ga}_{0.75}\text{As}$ layer thicknesses and from a sample containing only the 3 ML GaAs interlayer.

peak observed for $\text{In}_{0.25}\text{Ga}_{0.75}\text{As}$ thicknesses below 1.5 ML is not clear. The splitting may originate from monolayer-high thickness fluctuations of the GaAs and $\text{In}_{0.25}\text{Ga}_{0.75}\text{As}$ layers as observed in the AFM images in Figure 3.

The storage time of charge carriers within QDs can be determined by a method being analogous to DLTS. We investigate the temperature dependence of the decay transient of the capacity of a pn junction with embedded QD layers.¹⁶ Suitable pn-diode structures are realized by inserting a layer of $\text{In}_{0.25}\text{Ga}_{0.75}\text{As}$ QDs in the low p-doped region of a pn junction. The epitaxial structure is described in the inset of Figure 5. A sample containing the 3 ML GaAs interlayer but no QD layer, and a sample comprising only the pn junction are studied as references. The localization centers are initially charged with hole charge carriers by supplying a 100 ms forward voltage pulse to the diodes at a steady bias of 0 V. The capacitance transients are taken afterwards at a reversed bias of 4 V. The DLTS signal resulting from the emission transients is shown in Figure 5 for a reference time constant of 483 ms. A large peak around 190 K can be seen for the QD sample, while the feature is missing in both reference samples. All three samples show a peak around 300 K, which is attributed to a defect state in GaP. An Arrhenius plot yields a mean activation energy of 489 meV for the QD peak with a capture cross section of $4.4 \times 10^{-13} \text{ cm}^2$. The second peak in all three samples has a mean activation energy between 650 meV and 690 meV with a capture cross section between 2 and $4 \times 10^{-15} \text{ cm}^2$. The QD capture cross section of $4.4 \times 10^{-13} \text{ cm}^2$ measured here lies within the range of typical QD capture cross sections, i.e., $7.0 \times 10^{-12} \text{ cm}^2$ for $\text{In}_{0.8}\text{Ga}_{0.2}\text{As}/\text{GaAs}$ QDs¹⁶ and $7.0 \times 10^{-16} \text{ cm}^2$ for GaSb/GaAs QDs.¹⁷ Eight-band $\mathbf{k} \cdot \mathbf{p}$ calculations¹⁸ for strained truncated pyramidal $\text{In}_{0.25}\text{Ga}_{0.75}\text{As}$ QDs yield a hole localization energy of 462 meV assuming 3 ML height. This result is in good agreement with the measured activation energy. From the activation energy and the capture cross section, the storage time of holes at room temperature is estimated to 3 μs .

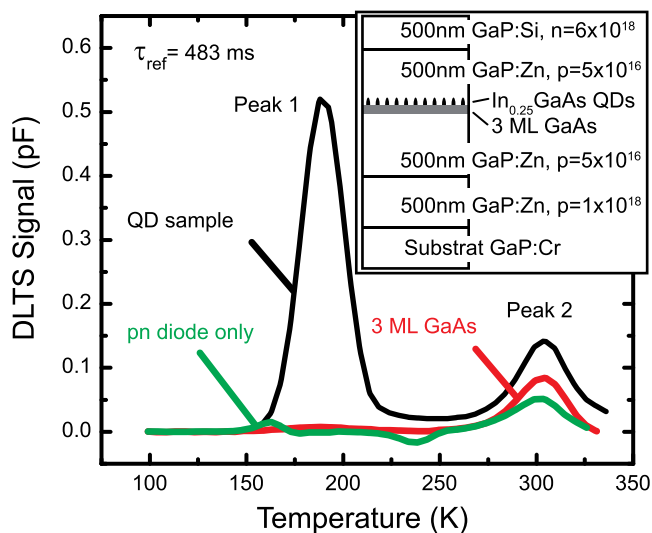


FIG. 5. DLTS spectra of hole capture. The pulse length and reference time constant were set to 100 ms and 483 ms, respectively. The inset shows the structure of the pn-diode.

In conclusion, SK growth of $\text{In}_{0.25}\text{Ga}_{0.75}\text{As}$ layers on GaP(001) is achieved by reducing the surface energy of the GaP substrate using a 3 ML GaAs interlayer. The critical layer thickness for QD formation lies between 0.75 ML and 1.0 ML of $\text{In}_{0.25}\text{Ga}_{0.75}\text{As}$. QD formation is also seen in CL measurements where the $\text{In}_{0.25}\text{Ga}_{0.75}\text{As}$ related emission red-shifts by 65 meV when the critical layer thickness is exceeded. A mean activation energy of 489 meV for holes trapped in these QDs with a capture cross section of $4.4 \times 10^{-13} \text{ cm}^2$ is measured by DLTS, yielding a hole storage time of 3 μs .

The authors thank M. Dähne for fruitful discussion of the manuscript, B. Jaeger, Irina A. Ostapenko, D. Roy, and J. Schuppang for help with the experiments, and the DFG, Contract No. BI284/29-1 and SFB 787 TPA4, the Federal Ministry of Economics and Technology (BMW) Grant. No. 03VWP0059v and the Federal Ministry of Education and Research, Grant No. 16V0196 (HOFUS).

¹F. Heinrichsdorff, M.-H. Mao, N. Kirstaedter, A. Krost, D. Bimberg, A. O. Kosogov, and P. Werner, *Appl. Phys. Lett.* **71**, 22 (1997).

²H. Moriya, Y. Nonogaki, S. Fuchi, A. Koizumi, Y. Fujiwara, and Y. Takeda, *Microelectron. Eng.* **51–52**, 35 (2000).

- ³R. Leon, C. Lobo, T. P. Chin, J. M. Woodall, S. Fafard, S. Ruvimov, Z. Liliental-Weber, and M. A. S. Kalceff, *Appl. Phys. Lett.* **72**, 1356 (1998).
- ⁴Y. Song, P. J. Simmonds, and M. L. Lee, *Appl. Phys. Lett.* **97**, 223110 (2010).
- ⁵T. Nguyen Thanh, C. Robert, C. Cornet, M. Perrin, J. M. Jancu, N. Bertru, J. Even, N. Chevalier, H. Folliot, O. Durand, and A. Le Corre, *Appl. Phys. Lett.* **99**, 143123 (2011).
- ⁶A. Marent, T. Nowozin, M. Geller, and D. Bimberg, *Semicond. Sci. Technol.* **26**, 014026 (2011).
- ⁷M. Geller, E. Stock, C. Kapteyn, R. Sellin, and D. Bimberg, *Phys. Rev. B* **73**, 205331 (2006).
- ⁸L. Pedesseau, J. Even, A. Bondi, W. Guo, S. Richard, H. Folliot, C. Labbe, C. Cornet, O. Dehaese, A. L. Corre, O. Durand, and S. Loualiche, *J. Phys. D: Appl. Phys.* **41**, 165505 (2008).
- ⁹M. Grundmann, O. Stier, and D. Bimberg, *Phys. Rev. B* **52**, 11969 (1995).
- ¹⁰I. N. Stranski and L. Krastanow, *Monatshefte Chem.* **71**, 351 (1937).
- ¹¹V. Shchukin and D. Bimberg, *Rev. Mod. Phys.* **71**, 1125 (1999).
- ¹²C. Messmer and J. C. Bilello, *J. Appl. Phys.* **52**, 4623 (1981).
- ¹³J. W. Cahn and R. E. Hanneman, *Surf. Sci.* **1**, 387 (1964).
- ¹⁴A. Lenz, R. Timm, H. Eisele, C. Hennig, S. K. Becker, R. L. Sellin, U. W. Pohl, D. Bimberg, and M. Daehne, *Appl. Phys. Lett.* **81**, 5150 (2002).
- ¹⁵H. Eisele and M. Dähne, *J. Cryst. Growth* **338**, 103 (2012).
- ¹⁶M. Geller, A. Marent, E. Stock, D. Bimberg, V. I. Zubkov, I. S. Shulgunova, and A. V. Solomonov, *Appl. Phys. Lett.* **89**, 232105 (2006).
- ¹⁷T. Nowozin, A. Marent, L. Bonato, A. Schliwa, D. Bimberg, E. Smakman, J. Garleff, P. Koenraad, R. Young, and M. Hayne, *Phys. Rev. B* **86**, 035305 (2012).
- ¹⁸A. Schliwa, M. Winkelkemper, and D. Bimberg, *Phys. Rev. B* **76**, 205324 (2007).